EPJ Web of Conferences **276**, 01021 (2023) https://doi.org/10.1051/epjconf/202327601021
SQM 2022

Proton and Λ flow and the equation of state at high density

Jan Steinheimer[1,*], *Manjunath* Omana Kuttan[1,2,3], *Anton* Motornenko[1], *Agnieszka* Sorensen[4], *Yasushi* Nara[5], *Volker* Koch[6], *Marcus* Bleicher[2,7,8], and *Horst* Stoecker[1,2,7]

[1]Frankfurt Institute for Advanced Studies, Ruth-Moufang-Str. 1, D-60438 Frankfurt am Main, Germany
[2]Institut für Theoretische Physik, Goethe Universität Frankfurt, Max-von-Laue-Str. 1, D-60438 Frankfurt am Main, Germany
[3]Xidian-FIAS international Joint Research Center, Giersch Science Center, D-60438 Frankfurt am Main, Germany
[4]Institute for Nuclear Theory, University of Washington, Box 351550, Seattle, Washington 98195, USA
[5]Akita International University, Yuwa, Akita-city 010-1292, Japan
[6]Lawrence Berkeley National Laboratory, 1 Cyclotron Road, Berkeley, California 94720, USA
[7]GSI Helmholtzzentrum für Schwerionenforschung GmbH, Planckstr. 1, D-64291 Darmstadt, Germany
[8]Helmholtz Research Academy Hesse for FAIR (HFHF), GSI Helmholtzzentrum für Schwerionenforschung GmbH, Campus Frankfurt, Max-von-Laue-Str. 12, 60438 Frankfurt am Main, Germany

Abstract. Results on proton and Λ flow, calculated with the UrQMD model that incorporates different realistic density dependent equations of state, are presented. It is shown that the proton and hyperon flow shows sensitivity to the equation of state and especially to the appearance of a phase transition at densities below $4n_0$. Even though qualitatively hyperons and protons exhibit the same beam energy dependence of the flow, the quantitative results are different. In this context it is suggested that the hyperon measurements can be used to study the density dependence of the hyperon interaction in high density QCD matter.

1 Introduction

The properties of high density strongly interacting matter can be studied in large collider experiments where heavy nuclei are smashed at relativistic energies to create the densest and hottest matter observed in the universe. At the same time, new astrophysical observatories allow us to study the collisions of the densest macroscopic objects, neutron stars, as binary neutron star mergers (BNSM) which create matter that shows remarkable similarities with the matter created in heavy ion collisions [1–3]. In terrestrial experiments at the RHIC as well as the planned facilities at GSI/FAIR and HIAF, systems created in microscopic collisions of heavy nuclei can now be studied with unprecedented accuracy and statistics. One of the main open challenges in the physics of the strong interaction, Quantum Chromo Dynamics (QCD), is the possibility of a phase transition in matter at densities above twice nuclear saturation density. For systems with vanishing net baryon number and high temperatures, first principle lattice QCD calculations have converged to a picture of a smooth crossover from a hadronic system to a dense state of matter where chiral symmetry is restored [4, 5].

*e-mail: steinheimer@fias.uni-frankfurt.de

Since these simulations at finite baryon density suffer from the fermionic sign problem, no reliable predictions are yet possible for the range of moderate temperature up to $T < 150\,\mathrm{MeV}$ and densities above twice saturation density. In this region of the phase diagram one has to rely on comparing model simulations with a wealth of experimental data which is and will become available. Many observables have been proposed in the past to be sensitive probes for a possible phase transition. To get a consistent picture of the high density QCD equation of state (EoS), using the now available wealth of data, requires a model which is able to incorporate any possible high density EoS and allow us to compute the various observables. In this talk we presented such an approach where it is now possible to incorporate any density dependent EoS in the UrQMD transport model. First results of proton and hyperon flow and its dependence on the EoS and specifically a phase transition were presented. It was found that a phase transition at densities below four times nuclear saturation density is not consistent with available flow data.

2 CMF in UrQMD

To extend the current version of UrQMD [6, 7] and allow the implementation of any density dependent EoS (also with a phase transition) a simple method is used. Besides the cascade part, including elastic and inelastic scattering of many hadronic species, resonance excitations and decays as well as string formation and fragmentation, the UrQMD model includes a quantum molecular dynamics (QMD) part to describe the real part of the nucleon interactions [8]. In the QMD part, the change in the momenta of the baryons are due to a density-dependent potential and are calculated using non-relativistic Hamilton equations of motion:

$$\dot{\mathbf{p}}_i = -\frac{\partial \mathbf{H}}{\partial \mathbf{r}_i} = -\frac{\partial \mathbf{V}}{\partial \mathbf{r}_i} = -\left(\frac{\partial V_i}{\partial n_i} \cdot \frac{\partial n_i}{\partial \mathbf{r}_i}\right) - \left(\sum_{j \neq i} \frac{\partial V_j}{\partial n_j} \cdot \frac{\partial n_j}{\partial \mathbf{r}_i}\right), \tag{1}$$

where $n_{\{i,j\}} \equiv n_B(\boldsymbol{r}_{\{i,j\}})$ is the local interaction density of baryon i or j. Thus, V_i corresponds to the average potential energy of a baryon at position $\boldsymbol{r}_i$, and the local interaction density n_B at position $\boldsymbol{r}_k$ is calculated by assuming that each particle can be treated as a Gaussian wave packet [6, 8].

To implement any realistic EoS in the QMD part of the UrQMD model, we need to calculate the density dependence of the average field energy per baryon $V(n_B)$ within each model, which then can be used in the QMD equations of motion given by Eq. (1). In particular, $V(n_B)$ and its derivative need to be provided in order to numerically calculate changes in momentum at a given time-step. In the following we will use the chiral mean field model (CMF) developed in Frankfurt [9] to provide this density dependent potential. The CMF is based on a chiral mean field Lagrangian in which nucleons and their parity partners as well as quarks interact with the scalar and vector fields. In this approach properties of nuclear matter as well as deconfinement aspects and lattice QCD constraints can be incorporated simultaneously [10]. In the CMF model, the nucleon interaction is described relativistically via scalar and vector mean fields which are not present in UrQMD. Fortunately, the effective field energy per baryon E_{field}/A can be used, i.e., the relevant quantity which enters the equations of motion is then defined as

$$V_{\mathrm{CMF}} = E_{\mathrm{field}}/A \equiv E_{\mathrm{CMF}}/A - E_{\mathrm{FFG}}/A\,, \tag{2}$$

where E_{CMF}/A is the total energy per baryon at $T = 0$ from the CMF model and E_{FFG}/A is the energy per baryon in a free non-interacting Fermi gas.

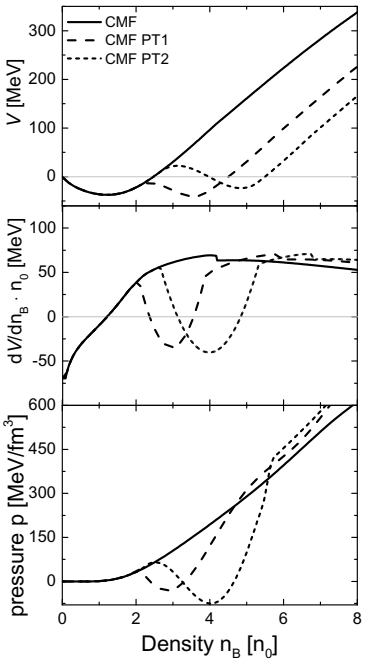

Figure 1. Upper panel: Potential energy per baryon as function of the net baryon density for the three QMD equations of state used in this study. PT1 and PT2 both contain a phase transition visible by the second minimum in the potential energy. Middle panel: Derivative of the potential energy with respect to the net baryon density. Lower panel: Pressure as function of baryon density, corresponding to the three equations of state used.

The resulting average field energy per baryon as a function of the baryon density, from the CMF model, is shown in the upper panel of Fig.1. Here, the original CMF model which incorporates only a crossover is compared with two extensions where an additional first order phase transition has been incorporated in the EoS, referred to as PT1 and PT2 (see [11] for a different method of expanding the potential that can incorporate a phase transition). The middle panel shows the derivative of the potential energy with respect to the baryon density as used in eq. 1 and the lower panel shows the thermodynamic pressure calculated with the given potential. The pressure represents the equation of state and the two phase transitions PT1 and PT2 can be clearly seen as dips in the pressure leading to unstable phases defined by the regions where the derivative of the pressure w.r.t. the density becomes negative. A detailed description of the implementation and details of the UrQMD+CMF model and how a phase transition can be included can be found in [12, 13].

To determine how well the UrQMD model with the CMF potential can describe the evolution of a hot fireball with given equation of state, we first compare the time dependence of bulk properties like the density and temperature of central collisions of Au nuclei at various beam energies. The UrQMD simulations with the standard CMF potential are contrasted with fully consistent relativistic fluid dynamic simulations that include also the CMF equation of state. The density can simply be calculated in the central volume of the collisions by averaging over many UrQMD events while the fluid dynamic simulation was initialized with a smooth initial condition of two cold and Lorenz contracted counterstreaming nuclei.

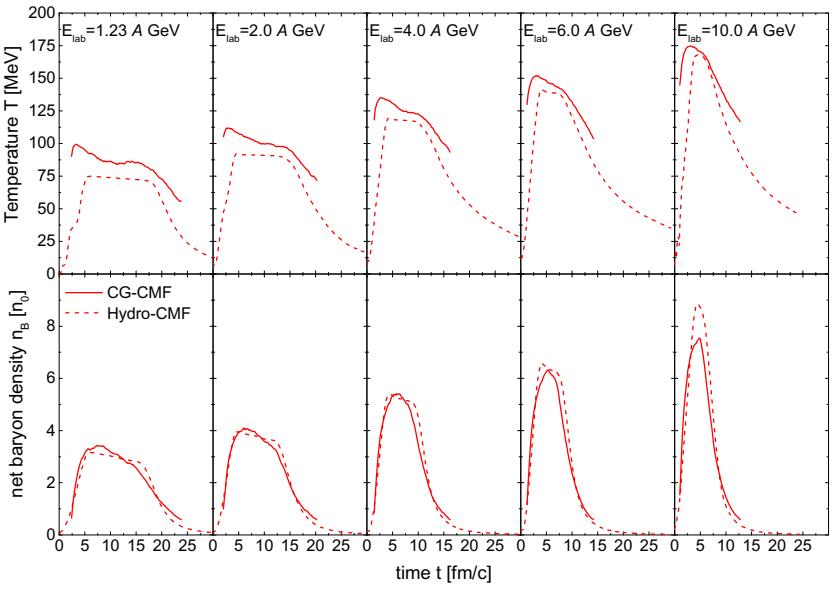

Figure 2. Upper panels: Time evolution of the temperature in a central volume for Au-Au collisions various beam energies calculated in a fully relativistic 3+1D 1-fluid dynamical simulation (dashed lines) and the UrQMD-CMF simulations (solid lines). Lower panels: Time evolution of the central net baryon density in the same systems. All simulations use the CMF-EoS as input [13].

The temperature can also be extracted directly from the CMF EoS included in the fluid simulation. In the UrQMD-CMF simulation, first the averaged energy and momentum density have to be calculated and can then be related to the corresponding temperature in the CMF EoS. The details on the procedure are described in [13]. Figure 2 shows the time evolution for the temperature (upper panels) and net baryon density (lower panels) for different kinetic beam energies in the laboratory frame. The UrQMD simulations (solid lines) are compared to the full fluid dynamic simulations (dashed lines). One can clearly see that the highest compression, which is strongly affected by the EoS used, is almost identical for the two different dynamical descriptions. Also the Temperature is similar. However, the non-equilbrium UrQMD approach leads to slightly larger temperatures. This result shows that indeed the UrQMD-CMF implementation leads to bulk matter compressions expected for this equation of state from a fully consistent fluid model. It is therefore expected that also other quantities can be consistently described by this non-equilibrium approach which has the advantage that no ad-hoc procedures for the fluidization and particlization process are required. In the following we will make use of this and calculate different flow coefficients using the CMF EoS with and without a phase transition and compare them to available data.

Figure 3 presents (from top to bottom) the excitation functions of the (mid-rapidity) mean transverse kinetic energy, the elliptic flow and the slope of the directed flow for protons as well as Λ's, simulated with the UrQMD model with 3 different equations of state. For all beam energies, we considered only Au-Au collisions at different centralities indicated in the figures. The solid lines correspond to the results obtained with the standard CMF-EoS and the dashed lines represent the two different phase transitions. All observables show a clear dependence on the equation of state. The mean transverse kinetic energy increases

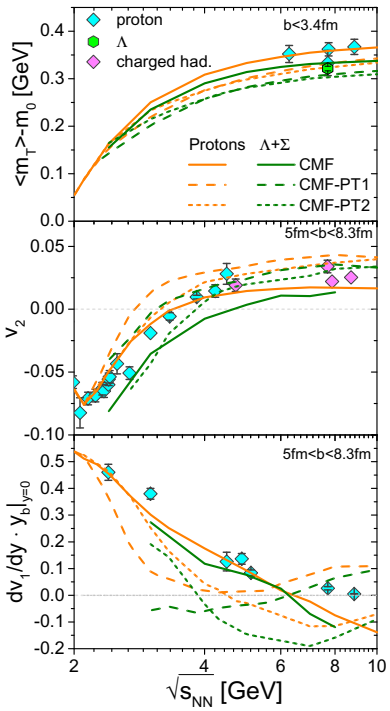

Figure 3. Upper panel: Mean transverse mass of protons (orange) and Λ's (green) in central Au-Au collisions at various beam energies compared to proton and Λ data [14–16]. Middle panel: Elliptic flow v_2 of protons (orange) and Λ's (green) in mid-central Au-Au collisions at various beam energies compared to proton data [17–23]. Lower panel: Slope of the directed flow v_1 of protons (orange) and Λ's (green) in mid-central Au-Au collisions at various beam energies compared to proton data [21–28].

for a stiffer EoS, the elliptic flow (calculated with respect to the reaction plane) shows an opposite behavior and increases for a softer EoS. The slope of the directed flow v_1 even shows a clear minimum for the scenarios with a phase transition as predicted from fluid dynamic simulations [29]. Regarding the hyperon flow we also observe the same effects as for the protons qualitatively, however, all hyperon flow components appear to be reduced compared to the protons. Compared to the available data on proton flow, the standard CMF-EoS provides the best description of the data.

3 Discussion

Results on the sensitivity of proton and hyperon flow on the equation of state in the UrQMD approach were presented. It was shown that the EoS and especially the presence of a phase transition at densities below $4n_0$ has significant impact on the observed flow of both protons and hyperons. Similar results have been obtained recently in [30]. In addition it was shown that, even though the QMD-potential used for protons and hyperons is identical, the flow is not. These findings are in line with a first study [31] where it was argued that Λ flow can be a sensitive probe for the hyperon interaction in dense nuclear matter. Our study, using a realistic density dependent potential consistent with astrophysical observations, confirms this

statement and can be seen as a first step into the study of hyperon interactions with UrQMD-CMF. In the future more detailed studies on hyperon flow may be useful tools to understand the hyperon interaction in dense matter found also in compact stars and their mergers.

A.M. acknowledges the Stern–Gerlach Postdoctoral fellowship of the Stiftung Polytechnische Gesellschaft. M.O.K. thanks GSI for funding. A.S. acknowledges support by the U.S. Department of Energy, Office of Science, Office of Nuclear Physics, under Grant No. DE-FG02-00ER41132. Y.N. acknowledges support by JSPS KAKENHI Grant Number JP21K03577. V.K. acknowledges support by the U.S. Department of Energy, Office of Science, Office of Nuclear Physics, under contract number DE-AC02-05CH11231. M.B. acknowledges support by the EU–STRONG 2020 network. The computational resources for this project were provided by the Center for Scientific Computing of the GU Frankfurt and the Goethe–HLR.

References

[1] A. Bauswein, S. Goriely and H. T. Janka, Astrophys. J. **773**, 78 (2013).
[2] M. Hanauske, J. Steinheimer, L. Bovard, A. Mukherjee, S. Schramm, K. Takami, J. Papenfort, N. Wechselberger, L. Rezzolla and H. Stöcker, J. Phys. Conf. Ser. **878**, no.1, 012031 (2017).
[3] E. R. Most, A. Motornenko, J. Steinheimer, V. Dexheimer, M. Hanauske, L. Rezzolla and H. Stoecker, [arXiv:2201.13150 [nucl-th]].
[4] S. Borsanyi, Z. Fodor, C. Hoelbling, S. D. Katz, S. Krieg and K. K. Szabo, Phys. Lett. B **730**, 99-104 (2014).
[5] A. Bazavov *et al.* [HotQCD], Phys. Rev. D **90**, 094503 (2014).
[6] S. A. Bass, M. Belkacem, M. Bleicher, M. Brandstetter, L. Bravina, C. Ernst, L. Gerland, M. Hofmann, S. Hofmann and J. Konopka, *et al.* Prog. Part. Nucl. Phys. **41**, 255-369 (1998).
[7] M. Bleicher, E. Zabrodin, C. Spieles, S. A. Bass, C. Ernst, S. Soff, L. Bravina, M. Belkacem, H. Weber and H. Stoecker, *et al.* J. Phys. G **25**, 1859-1896 (1999).
[8] J. Aichelin, Phys. Rept. **202**, 233-360 (1991).
[9] A. Motornenko, S. Pal, A. Bhattacharyya, J. Steinheimer and H. Stoecker, Phys. Rev. C **103**, 054908 (2021).
[10] J. Steinheimer, S. Schramm and H. Stöcker, Phys. Rev. C **84**, 045208 (2011).
[11] A. Sorensen and V. Koch, Phys. Rev. C **104**, no.3, 034904 (2021).
[12] J. Steinheimer, A. Motornenko, A. Sorensen, Y. Nara, V. Koch and M. Bleicher, Eur. Phys. J. C **82** (2022) no.10, 911.
[13] M. Omana Kuttan, A. Motornenko, J. Steinheimer, H. Stoecker, Y. Nara and M. Bleicher, Eur. Phys. J. C **82**, no.5, 427 (2022).
[14] C. Alt *et al.* [NA49], Phys. Rev. C **73**, 044910 (2006).
[15] L. Adamczyk *et al.* [STAR], Phys. Rev. C **96**, no.4, 044904 (2017).
[16] J. Adam *et al.* [STAR], Phys. Rev. C **102**, no.3, 034909 (2020).
[17] C. Pinkenburg *et al.* [E895], Phys. Rev. Lett. **83**, 1295-1298 (1999).
[18] D. Adamova *et al.* [CERES], Nucl. Phys. A **698**, 253-260 (2002).
[19] A. Andronic *et al.* [FOPI], Phys. Lett. B **612**, 173-180 (2005).
[20] L. Adamczyk *et al.* [STAR], Phys. Rev. C **86**, 054908 (2012).
[21] J. Adam *et al.* [STAR], Phys. Rev. C **103**, no.3, 034908 (2021).
[22] J. Adamczewski-Musch *et al.* [HADES], Phys. Rev. Lett. **125**, 262301 (2020).
[23] M. S. Abdallah *et al.* [STAR], Phys. Lett. B **827**, 137003 (2022).
[24] M. S. Abdallah *et al.* [STAR], Phys. Lett. B **827**, 136941 (2022).

[25] J. Adamczewski-Musch *et al.* [HADES], [arXiv:2208.02740 [nucl-ex]].
[26] E. Kashirin *et al.* [NA61/Shine], J. Phys. Conf. Ser. **1690**, no.1, 012127 (2020).
[27] J. Barrette *et al.* [E877], Phys. Rev. C **55**, 1420-1430 (1997).
[28] C. Alt *et al.* [NA49], Phys. Rev. C **68**, 034903 (2003).
[29] H. Stoecker, Nucl. Phys. A **750**, 121-147 (2005).
[30] D. Oliinychenko, A. Sorensen, V. Koch and L. McLerran, [arXiv:2208.11996 [nucl-th]].
[31] Y. Nara, A. Jinno, K. Murase and A. Ohnishi, Phys. Rev. C **106** (2022) no.4, 4.